



Published in final edited form as:

Nat Cell Biol. 2009 September ; 11(9): 1121–1127. doi:10.1038/ncb1926.

## Organizer restriction through modulation of Bozozok stability by the E3 ubiquitin ligase Lnx-like

Hyunju Ro and Igor B. Dawid\*

Laboratory of Molecular Genetics, Eunice Kennedy Shriver National Institute of Child Health and Human Development, National Institutes of Health, Bethesda, Maryland, United States of America

### Abstract

The organizer anchors the primary embryonic axis, and balance between dorsal (organizer) and ventral domains is fundamental to body patterning. Ligand of Numb protein-X (LNX) is a RING finger and four PDZ domain containing E3 ubiquitin ligase<sup>1,2</sup>. LNX serves as a binding platform and may have a role in cell fate determination, but its *in vivo* functions are unknown<sup>1–5</sup>. Here we show that Lnx-1 (Lnx-like) acts as a critical regulator of dorso-ventral (D-V) axis formation in zebrafish. Depletion of Lnx-1 using specific antisense morpholinos (MO), caused strong embryonic dorsalization. We identified Bozozok (Boz; also called Dharma or Nieuwkoid) as a binding partner and substrate of Lnx-1. Boz is a homeodomain-containing transcriptional repressor induced by canonical Wnt signaling that is critical for dorsal organizer formation<sup>6–12</sup>. Lnx-1 induced K48-linked polyubiquitination of Boz, leading to its proteasomal degradation in human 293T cells and in zebrafish embryos. Dorsalization induced by Boz overexpression was suppressed by raising the level of Lnx-1, but Lnx-1 failed to counteract dorsalization caused by mutant Boz lacking a critical motif for Lnx-1 binding. Further, dorsalization induced by depletion of Lnx-1 was alleviated by attenuation of Boz expression. We conclude that Lnx-1 modulates Boz activity to prevent the invasion of ventral regions of the embryo by organizer tissue. These studies introduce a ubiquitin ligase, Lnx-1, as a balancing modulator of axial patterning in the zebrafish embryo.

---

A role for proteolysis in early embryogenesis was first suggested by the finding that degradation of  $\beta$ -catenin is selectively inhibited on the future dorsal side of the *Xenopus* embryo, marking the initial step in D-V axis specification<sup>13–15</sup>. Components similar to the SCF- $\beta$ -TrCP complex which mediates  $\beta$ -catenin destruction, also limit Xom/Vent2/Vox stability<sup>16</sup>. Further, the Smurf1 E3 ubiquitin ligase is involved in D-V patterning by mediating degradation of Smad1 and reducing BMP signaling<sup>17,18</sup>. While tight regulation of the levels of multiple proteins is undoubtedly required during early embryonic development, the involvement of E3 ubiquitin ligases besides the SCF- $\beta$ -TrCP complex and Smurf1 have not been reported to date.

---

Users may view, print, copy, and download text and data-mine the content in such documents, for the purposes of academic research, subject always to the full Conditions of use:[http://www.nature.com/authors/editorial\\_policies/license.html#terms](http://www.nature.com/authors/editorial_policies/license.html#terms)

\*Correspondence: idawid@nih.gov.

Three closely related Lnx homologues are expressed during zebrafish development (Lnx-1: BC124171, Lnx-2: FJ156085, Lnx-like: FJ156084, Supplementary Fig. 1, Supplementary Fig. 2). Among the Lnx homologues, *Lnx-like* is strongly expressed maternally, with zygotic expression starting around the onset of gastrulation in marginal blastomeres, exhibiting a ventral-to-dorsal gradient (Supplementary Fig. 2). To explore the embryonic role of Lnx-1, we inhibited its expression with antisense MOs which are effective in blocking *lnx-1* translation (Fig. 1a). Injection of UTR or ATG targeted MOs caused similar embryonic defects, displaying oval shape at early somitogenesis and degenerated tail and trunk at 24 hours post fertilization (hpf), both hallmarks of dorsalization (Fig. 1b–d, Supplementary Fig. 3). The dorsalized morphant phenotype was rescued by the co-injection of MO-resistant *lnx-1* mRNA (Supplementary Fig. 3). Since a splice blocking MO, expected to inhibit zygotic expression of Lnx-1, failed to induce dorsalization (data not shown), we conclude that maternal transcripts are responsible for the effect of Lnx-1 on D-V patterning. Dorsalization caused by Lnx-1 depletion was confirmed by analyzing several D-V markers. In the morphants, the organizer markers *gooseoid* (*gsc*) and *chordin* (*chd*) were expanded ventrolaterally at the expense of the expression domain of the ventral markers *vox* and *vent* (Fig. 1e–l). Likewise, the expression domains of neuroectodermal markers (*otx2* and *hoxb1b*) extended into ventral regions in the morphants (Fig. 1m and n). Overexpression of Lnx-1 caused axial mesoderm defects including anterior notochord and forebrain malformations and a shortened body axis, reminiscent of the strongest *boz* mutant phenotype<sup>8</sup> (Supplementary Fig. 4). These results indicate that maternal *lnx-1* transcripts are critical for D-V patterning of the embryo.

Since mammalian LNX acts as an E3 ubiquitin ligase<sup>1,2,19</sup>, we searched for potential target proteins by carrying out a yeast two-hybrid screen, and isolated a clone encoding a partial homeobox domain of *vent*. As full length Vent failed to bind to Lnx-1 (data not shown), we tested other homeobox genes expressed in the early embryo, and found strong interaction between Lnx-1 and Boz in the yeast two-hybrid system (Fig. 2a). Boz is a key regulatory factor in organizer formation in the embryo<sup>6–8,20</sup>. The physical interaction between Lnx-1 and Boz was verified by showing that epitope-tagged Boz and wild type Lnx-1, Lnx-1 Mu (conserved histidine and cysteine residues in the RING domain were replaced by alanine; H63A, C66A), and Lnx-1 N (carrying a RING domain deletion) could be co-immunoprecipitated using purified proteins *in vitro* (Fig. 2b) and in transfected cell lysates (Fig. 3a). Incubation of Boz and Lnx-1 isolated from cultured cells in an *in vitro* ubiquitination system (see Methods) produced ubiquitinated derivatives of Boz (Fig. 2c). No ubiquitination was seen when a RING domain mutant of Lnx-1 was used, or when the substrate was Boz All K/R, a mutant in which all five lysines in Boz were changed to arginines (Fig. 2c); lysine residues are the most common target sites, resulting in an isopeptide bond between ubiquitin and the substrate<sup>21</sup>.

As in the *in vitro* reaction, polyubiquitinated Boz was detected after cotransfection of Boz and Lnx-1 into cultured cells, and the expression level of Boz was reduced (Fig. 3a). Even though Boz All K/R did coprecipitate with Lnx-1, this mutant was not ubiquitinated in cultured cells (Fig. 3a), confirming the *in vitro* results (Fig. 2c). Additionally, Boz All K/R was not destabilized by Lnx-1 when injected into zebrafish embryos (Fig. 3g). To check the

specificity of the Boz-Lnx-1 interaction we tested whether Gsc, an organizer homeodomain protein and the closest homolog of Boz, could act as a substrate of Lnx-1. Binding between Gsc and Lnx-1 and polyubiquitination of Gsc by Lnx-1 were very weak and probably not significant as expression levels of Gsc were not substantially affected by co-transfection with Lnx-1 (Fig. 2d and e). These data indicate that Boz is a specific target of Lnx-1, and that the RING domain is important for ubiquitination of Boz by Lnx-1 but is dispensable for their physical interaction (Fig. 3a).

The Lnx-1-binding domains in Boz were mapped by testing deletion constructs, pointing to a critical region upstream of the homeodomain (Supplementary Fig. 5a and b). More detailed mapping of the binding domain in Boz identified amino acid (aa) residues 44–84 as essential (Fig. 3b). The aa 44–84 deletion mutant, Boz<sup>BD</sup>, will be used in biological experiments below. The aa 44–84 domain was necessary but not sufficient to interact with Lnx-1 (Fig. 3b; Supplementary Fig. 5c and d), indicating that additional domain(s) are required. Indeed, the C-terminal 15 amino acids of Boz are essential for efficient binding to Lnx-1 (Supplementary Fig. 5a and b).

Polyubiquitin chains have diverse structures due to the presence of seven lysine residues in ubiquitin<sup>21–23</sup>. Different chain conformations have different biological consequences, with K48-linked polyubiquitinated proteins usually undergoing 26S proteasome-dependent proteolysis. We examined the nature of Boz polyubiquitination by Lnx-1 by co-transfection of Boz with wild type or mutant ubiquitin constructs (Ub-K48R, Ub-K63R, Ub-K48/63R), all of which allow formation of a monoubiquitinated substrate but limit the type of polyubiquitin chain outgrowth. As shown in Figure 3c, K63R mutant ubiquitin was as effective as wild type in modification of Boz, while Ub-K48R or Ub-K48/63R were largely inactive. These results indicate that Boz ubiquitination by Lnx-1 leads to K48-linked chains. This fact is consistent with the observation that Boz degradation following co-transfection with Lnx-1 was blocked by the proteasome inhibitors MG132 and lactacystin (Fig. 3d). In zebrafish embryos, Boz levels increased after depleting endogenous Lnx-1, whereas *lnx-1* mRNA-injected embryos showed a dramatic reduction in the level of Boz protein (Fig. 3e–g, Supplementary Fig. 5e). This reduction depends on Lnx-1 E3 ubiquitin ligase activity as Lnx-1<sup>Mu</sup> or Lnx-1<sup>N</sup> failed to induce a similar lowering of Boz protein (Fig. 3g, Supplementary Fig. 5e). In addition, Boz<sup>All K/R</sup> levels were stable in the presence of Lnx-1, suggesting that Boz destabilization depends on polyubiquitin chain formation (Fig. 3g). These results indicate that Lnx-1 negatively regulates Boz levels by post-translational regulation, providing an explanation for the dorsalization observed after depletion of Lnx-1 from the embryo.

In our experiments we used the 6xMyc tag in binding studies because of its high sensitivity. However, we noted that Myc-tagged Boz became stabilized rather than undergoing proteasomal degradation after cotransfection with Lnx-1 (Fig. 2d). Further, 6xMyc-tagged Boz showed K63-linked polyubiquitin chain elongation, and Lnx-1 was able to polyubiquitinate 6xMyc-tagged Boz<sup>All K/R</sup> (data not shown). These observations suggest that lysine residues within the Myc tag served as targets for Lnx-1-mediated ubiquitination. Therefore we used the lysine-free T7 epitope (MASMTGGQQMG) in all ubiquitination experiments; as expected, T7-tagged Boz<sup>All K/R</sup> was resistant to Lnx-1 dependent

ubiquitination (Fig. 2c and Fig. 3a). These observations show that the lysine(s) in an epitope tag can serve as targets for E3 ubiquitin ligases, potentially endangering the conclusions derived from constructs with lysine-containing tags.

In the zebrafish embryo, *boz* activation by a Wnt/ $\beta$ -catenin signal<sup>11,12</sup> mediates organizer formation by suppressing the expression of ventralizing genes such as *bmp*, *vox* (*vega1*), *vent* (*vega2*) and *ved*<sup>20,24–29</sup>. The similarity of defects caused by Boz overexpression and Lnx-1 depletion, and of *boz* null mutation<sup>8,10</sup> and Lnx-1 gain-of-function, suggested to us that Lnx-1 counteracts Boz *in vivo* by ubiquitination-dependent destabilization. Therefore we tested functional interactions between these two factors by injecting *boz* mRNA, with or without *lnx-1* mRNA, into zebrafish embryos. Embryos injected with 1  $\mu$ g *boz* mRNA were strongly dorsalized as previously reported<sup>7</sup>, and this phenotype was reversed by co-injection of *lnx-1* in a dosage-dependent manner (Fig. 4a). Dorsalization was also tested by expansion of the *gsc* expression domain at gastrula. Ectopic *gsc* expression induced by *boz* (100% = G2-G4) was significantly suppressed by *lnx-1* (45% = G1), but not by *lnx-1*  $\Delta$  N (Fig. 4b). Functional interaction between Lnx-1 and Boz is also indicated by the synergy between low levels of Lnx-1 suppression and Boz overexpression (1 ng *lnx-1* MO: 13% = G2; 1  $\mu$ g *boz* mRNA: 22% = G4; 1 ng *lnx-1* MO + 1  $\mu$ g *boz* mRNA: 80% = G4) (Fig. 4b). We predicted that the Lnx-1 binding domain mutant, Boz $\Delta$ BD, should retain dorsalizing activity, as it contains an intact Goosecoid-Engrailed homology domain at its N-terminus (Fig. 4c)<sup>6</sup>. We found that Boz $\Delta$ BD induced dorsalization more effectively than the wild type, and that this phenotype was resistant to co-injection with *lnx-1* or *lnx-1*  $\Delta$  N mRNA (Fig. 4d). As shown in Fig. 4e, Boz $\Delta$ BD was only very weakly polyubiquitinated by Lnx-1 and showed a stable expression level in the presence of Lnx-1.

Next we investigated the genetic interaction between *boz* and *lnx-1*. Since the expression levels of two *boz* target genes (*vent* and *vox*)<sup>25–27</sup> decreased through development in *lnx-1* morphants (Supplementary Fig. 6a–s), we tested whether this gradual reduction is a consequence of a reciprocal increase in *boz* expression. The initial level and range of *boz* expression was not affected in *lnx-1* morphants (Fig. 5a and b), but the *boz* expression domain was expanded by late blastula stage (Fig. 5c and d). Likewise, gradual expansion of *gsc* and *chd* was seen in the morphants (Supplementary Fig. 6t–e'). To explore whether dorsalization of *lnx-1* morphants could be restored by depletion of endogenous *boz*, we designed a splicing MO against *boz*. This MO specifically and efficiently blocked normal splicing of *boz*, strongly suppressed *noggin1* expression<sup>30</sup>, and affected shield formation (Supplementary Fig. 6f'–m'). Knockdown of *boz* rescued the embryonic dorsalized phenotype obtained by Lnx-1 depletion (Fig. 5e–g). In addition, ectopic *gsc* expression in the *lnx-1* morphants was alleviated in the *boz*-*lnx-1* double morphants (Fig. 5h–k). These data provide genetic evidence that *lnx-1* MO-dependent embryonic dorsalization can be suppressed by the attenuation of Boz expression.

Boz is a strong transcriptional repressor that is expressed transiently during early embryonic development<sup>6,7,20,25–27</sup>. This temporally restricted expression suggests that *boz* should be tightly regulated at the transcriptional and post-transcriptional level. Here we provide evidence for post-translational regulation of Boz. We propose that Lnx-1 regulates the output of early Wnt signaling by limiting the duration and range of Boz activity (Fig. 5l). It is

possible that *LnX-1* modulates early body patterning by affecting other molecules in addition to *Boz* because the *lnx-1* morphant phenotype could not be rescued completely by *boz* depletion, and the gain-of-function of *lnx-1* caused stronger embryonic malformations than the *boz* null mutation. However, regulation of *Gsc* does not appear to be involved as *LnX-1* neither binds nor ubiquitinates *Gsc* to a substantial extent (Fig. 2d and e). Our data indicate that the *LnX-1/Boz* interaction constitutes the major mechanism by which *LnX-1* limits the size of the organizer domain in the zebrafish embryo. The data presented here represent evidence that not only  $\beta$ -catenin but a direct target molecule of  $\beta$ -catenin signaling is down-regulated by the action of a specific E3 ubiquitin ligase to achieve patterning of the D-V body axis during early embryonic development.

## METHODS

### Yeast two-hybrid screening

The pAS2-1 and pGAD10 plasmids (Clontech) encode the GAL-4 DNA binding domain and the transcriptional activation domain. *LnX-1* open reading frame (ORF) fused to the GAL-4 DNA binding domain was generated by PCR cloning. cDNA libraries from zebrafish and *Xenopus* embryos were purchased from Clontech, and screening was performed according to the manufacturer's instructions. pAS2-1/*LnX-1* ORF and each cDNA library were cotransformed into the CG1945 yeast strain. Approximately  $1.4 \times 10^8$  *Xenopus* and  $4.5 \times 10^7$  zebrafish independent clones were screened. In interaction experiments (Fig. 2a), the same yeast strain was used, and mock refers to transfection with the corresponding empty vectors.

### Cell culture and Transfection

Cos7 and 293T cells were grown in Dulbecco's Modified Eagle's medium (DMEM) supplemented 10% fetal bovine serum (FBS). Cells in plates were transfected with various plasmid constructs by FuGene6 (Roche). After 24–48 hr, cells were harvested and the cell lysates were used for further assay.

### Immunoprecipitation and Western blotting

Cells were lysed by M-PER Mammalian Protein Extraction Reagent (Pierce) containing Complete protease inhibitor cocktail (Roche), and mixed with 15  $\mu$ l of Protein G Sepharose 4 Fast Flow (GE Healthcare). The total volume of lysate was adjusted to 800  $\mu$ l with NP-40 buffer (150 mM NaCl, 0.02%  $\text{NaN}_3$ , Complete protease inhibitor cocktail (Roche), 10 mM Tris-Cl, pH 7.2, 0.5% NP-40, 1 mM DTT). Precipitates were washed at least three times with ice-cold NP-40 buffer (1 ml), and were analyzed by Western blotting. In order to analyze polyubiquitination, immunoprecipitation used high stringency conditions (150 mM NaCl, 0.02%  $\text{NaN}_3$ , Complete protease inhibitor cocktail (Roche), 10 mM Tris-Cl, pH 7.2, 0.5% NP-40, 0.1% SDS, 1% sodium deoxycholate, 1 mM DTT). After separation in 12% Nu-PAGE (Invitrogen) and transfer to PVDF membranes, membranes were incubated for 1 hr in blocking solution (4% skim milk in Tris-buffered saline with 0.05% Tween-20) at room temperature, incubated with primary antibodies for 1 hr, followed by incubation with HRP-conjugated secondary antibody (Jackson, 1:1000 – 1:10000) for 1 hr. Detection used the ECL detection system (Pierce). Embryonic lysates were obtained by adding 10  $\mu$ l

CompLysis Protein Extraction Reagent (SignaGen) per embryo. Antibodies were obtained from Roche (rat HA), Sigma (mouse Flag), Calbiochem (mouse T7, mouse T7-HRP conjugate,  $\alpha$ -tubulin), Clontech (mouse Myc) and Millipore (rabbit Myc).

### Whole mount in situ hybridization

Antisense riboprobes were generated using the appropriate RNA polymerase following manufacturers' instructions (Roche). Hybridization signal was detected using pre-absorbed anti-digoxigenin-AP Fab fragment (Roche) diluted (1:2000) in blocking solution.

### In vitro translation

*In vitro* translation reactions were performed using TNT T7 Coupled Reticulocyte Lysate (Promega). We subcloned the *Lnx-1* ORF including the 5' untranslated region (UTR) into the modified pcGlobin231 vector to construct the template.

### Site directed mutagenesis

For amino acid substitution in *Lnx-1* H63A/C66A, a mega-primer was generated by PCR using *TLA* polymerase (Bioneer Inc.) (forward primer; 5'-GGGATCCGCCATGACGGAGTCTAAGACGTCTTCACTGCCG-3', reverse primer; 5'-GAGGCACTGGAAGGCATAAGTGGCGCCGCACAATGTG-3', mutated sequences underlined). The resulting mega-primer together with another primer (5'-GCTCGAGTTAAACCAGACTGCCAGGCCAGGAGACCACGG-3') were used to PCR-amplify the full length mutant *lnx-1*, which was subcloned into T-vector (pGEM-T Easy Vector Systems; Promega). Lysine free Boz mutant was generated by substitution of amino acids 5, 43, 164, 171 and 179 to arginine using the aforementioned mega-priming method.

### Boz deletion constructs

Internal deletion constructs of Boz were generated using a PCR-based method. For example, Boz BD was generated using four primers. P1: 5'-GATGAATTCGAACATGGCAACTCAGAAGTTTTTC3'; P2: 5'-CCCTGCATAGTAAGTCGACTTTTCTCAAGTGCCCCTG-3'; P3: 5'-CAGGGGCACTTGAGAAAGTCGACTTACTATGCAGGG-3' and P4: 5'-GATCTCTAGACTAATCTGATTCCTGATGATC-3'. Primary PCR reactions were carried out with two different sets of primers (P1 + P2 and P3 + P4) using PfuUltra DNA polymerase (Stratagene). Each PCR product was purified, mixed with the complementary product, and used as template in the second PCR reaction with P1 and P4 primers.

### mRNA and MO Microinjection

For microinjection, cDNA for *lnx-1*, *lnx-1 N*, *boz* and *boz BD* were individually subcloned into the pCS2+ or modified pCS2+ vector. mRNAs were synthesized from linearized constructs using the mMACHINE kit (Ambion Inc.) according to the manufacturer's instruction. After purification following the manufacturer's recommendation, mRNAs were dissolved in DEPC treated 0.1 M KCl. mRNAs and MOs were pressure injected into the yolk of 1–4 cell stage embryos. In order to reduce the p53 dependent off-targeting effect of MOs (*lnx-1* ATG MO and *lnx-1* splicing MO), we

coinjecting the MOs with a p53 MO32. Three different MOs against *lnx-1* and one *boz* splice-blocking MO were obtained from Gene Tools, LLC.

*Lnx-1* UTR MO: CCTACGCCTCTTTCACAGCTCACAA.

*Lnx-1* ATG MO: AGACTCCGTCATGGCCTGGAGAAGT.

*Lnx-1* splicing MO: GTAAGTGATGCAATACCATCTTCGC.

*Boz* splicing MO: AAATTGAAAATGCATACCGGCTACG.

### In vitro binding assay

BL21 (DE3) *E. coli* cells (Invitrogen) were used for expression of GST, GST-tagged Boz and S-tagged Lnx-1. The *boz* ORF was subcloned into the pGEX4T-1 (GE Healthcare Life Science), and *lnx-1* or *lnx-1* Mu was subcloned into pET29a (+) (Novagen). After adding IPTG (final concentration 1 mM), the bacteria were cultured for 2 h at 30° C, and lysed with B per solution (Pierce). The fusion proteins were purified as inclusion bodies, and were denatured and renatured using Rapid GST Inclusion Body Solubilization and Renaturation Kit (Cell Biolabs, Inc.) following the manufacturer's instruction.

Purified GST or GST-Boz was incubated with S-tagged Lnx-1 and Glutathione Sepharose 4 Fast Flow (GE Healthcare Life Science) for 2 h at 4°C with gentle agitation. Mixtures were then centrifuged and pellets were washed four times with ice-cold NP-40 buffer (150 mM NaCl, 0.02% NaN<sub>3</sub>, Complete protease inhibitor cocktail (Roche), 10 mM Tris-Cl, pH 7.2, 0.5% NP-40, 1 mM DTT). Bound proteins were eluted by boiling after adding 30 µl of gel loading buffer. Eluted proteins were separated by SDS-PAGE (12%), transferred to PVDF membrane, and S-tagged Lnx-1 was detected by immunoblotting using anti-S-tag antibody (Novagen) and chemiluminescent detection system (Pierce).

### In vitro ubiquitination assay

Expression constructs for 3xT7-Boz, 3xT7-Boz All K/R, Flag-Lnx-1 and Flag-Lnx-1 Mu were transfected into separate plates of 293T cells. Each culture was lysed, and nuclear fractions were isolated from Boz transfectants, while cytoplasmic fractions were isolated from Lnx-1 transfectants. Extracts were combined in various combinations (see Fig. 2c), and subjected to IP with anti-T7 antibody. After washing several times with IP buffer, the protein-bound beads were directly used for the *in vitro* ubiquitination assay. The beads were incubated with the components of the ubiquitination machinery which includes biotinylated ubiquitin, following the manufacturer's instructions (Ubiquitylation Kit, BIOMOL). As E2 we used UbcH5b, which proved the most effective among those tested (UbcH1, UbcH2, UbcH5a, UbcH5b, UbcH5c, UbcH8 and Ubc13). After 1 h incubation at 37°C, the reaction was terminated by adding IP buffer containing SDS (0.5%; final concentration). The reacted mixtures were heated for 5 min at 80°C in order to reliably dissociate Boz from Lnx-1 or any other potential interacting protein. After adding 1 ml of ice-cold IP buffer, 15 µl of fresh protein G sepharose beads and anti-T7 antibody, T7-tagged Boz or Boz All K/R proteins were recovered after 4 h incubation at 4°C with gentle agitation. After gel electrophoresis,

biotin-labeled ubiquitinated Boz was detected using the VECTASTAIN ABC Kit (Vector Laboratories, Inc.) and SuperSignal West Dura Extended Duration Substrate (Pierce).

## Supplementary Material

Refer to Web version on PubMed Central for supplementary material.

## Acknowledgments

We thank Mark Rath and John Gonzales for help with fish maintenance, and Dr. Seok-Yong Choi, Chonnam National University Medical School, Republic of Korea, for helpful comments. This work was supported by the Intramural Research Program of the NICHD, NIH.

## REFERENCES

1. Dho SE, et al. The mammalian numb phosphotyrosine-binding domain. Characterization of binding specificity and identification of a novel PDZ domain-containing numb binding protein LNX. *J. Biol. Chem.* 1998; 273:9179–9187. [PubMed: 9535908]
2. Nie J, et al. LNX functions as a RING type E3 ubiquitin ligase that targets the cell fate determinant Numb for ubiquitin-dependent degradation. *EMBO J.* 2002; 21:93–102. [PubMed: 11782429]
3. Sollerbrant K, et al. The Coxsackievirus and adenovirus receptor (CAR) forms a complex with the PDZ domain-containing protein ligand-of-numb protein-X (LNX). *J. Biol. Chem.* 2003; 278:7439–7444. [PubMed: 12468544]
4. Kansaku A, et al. Ligand-of-Numb protein X is an endocytic scaffold for junctional adhesion molecule 4. *Oncogene.* 2006; 25:5071–5084. [PubMed: 16832352]
5. Rice DS, Northcutt GM, Kurschner C. The Lnx family proteins function as molecular scaffolds for Numb family proteins. *Mol. Cell Neurosci.* 2001; 18:525–540. [PubMed: 11922143]
6. Koos DS, Ho RK. The *nieuwkoid* gene characterizes and mediates a Nieuwkoop-center-like activity in the zebrafish. *Curr. Biol.* 1998; 8:1199–1206. [PubMed: 9811602]
7. Yamanaka Y, et al. A novel homeobox gene, *dharma*, can induce the organizer in a non-cell-autonomous manner. *Genes Dev.* 1998; 12:2345–2353. [PubMed: 9694799]
8. Fekany K, et al. The zebrafish *bozozok* locus encodes *Dharma*, a homeodomain protein essential for induction of gastrula organizer and dorsoanterior embryonic structures. *Development.* 1999; 126:1427–1438. [PubMed: 10068636]
9. Shimizu T, et al. Cooperative roles of *Bozozok/Dharma* and *Nodal*-related proteins in the formation of the dorsal organizer in zebrafish. *Mech. Dev.* 2000; 91:293–303. [PubMed: 10704853]
10. Solnica-Krezel L, Driever W. The role of the homeodomain protein *Bozozok* in zebrafish axis formation. *Int. J. Dev. Biol.* 2001; 45:299–310. [PubMed: 11291860]
11. Ryu SL, et al. Regulation of *dharma/bozozok* by the Wnt pathway. *Dev. Biol.* 2001; 231:397–409. [PubMed: 11237468]
12. Leung T, Söll I, Arnold SJ, Kemler R, Driever W. Direct binding of *Lef1* to sites in the *boz* promoter may mediate pre-midblastula-transition activation of *boz* expression. *Dev. Dyn.* 2003; 228:424–432. [PubMed: 14579381]
13. Larabell CA, et al. Establishment of the dorso-ventral axis in *Xenopus* embryos is presaged by early asymmetries in *beta*-catenin that are modulated by the Wnt signaling pathway. *J. Cell Biol.* 1997; 136:1123–1136. [PubMed: 9060476]
14. Miller JR, et al. Establishment of the Dorsal–Ventral Axis in *Xenopus* Embryos Coincides with the Dorsal Enrichment of Dishevelled That Is Dependent on Cortical Rotation. *J. Cell Biol.* 1999; 146:427–437. [PubMed: 10427095]
15. Liu J, et al. *Siah-1* mediates a novel *beta*-catenin degradation pathway linking *p53* to the adenomatous polyposis coli protein. *Mol. Cell.* 2001; 7:927–936. [PubMed: 11389840]
16. Zhu Z, Kirschner M. Regulated proteolysis of *Xom* mediates dorsoventral pattern formation during early *Xenopus* development. *Dev. Cell.* 2002; 3:557–568. [PubMed: 12408807]

17. Zhu H, Kavsak P, Abdollah S, Wrana JL, Thomsen GH. A SMAD ubiquitin ligase targets the BMP pathway and affects embryonic pattern formation. *Nature*. 1999; 400:687–693. [PubMed: 10458166]
18. Podos SD, Hanson KK, Wang YC, Ferguson EL. The DSmurf ubiquitin-protein ligase restricts BMP signaling spatially and temporally during *Drosophila* embryogenesis. *Dev. Cell*. 2001; 1:567–578. [PubMed: 11703946]
19. Weiss A, Baumgartner M, Radziwill G, Dennler J, Moelling K. c-Src is a PDZ interaction partner and substrate of the E3 ubiquitin ligase Ligand-of-Numb protein X1. *FEBS Lett*. 2007; 581:5131–5136. [PubMed: 17936276]
20. Leung T, et al. bozozok directly represses *bmp2b* transcription and mediates the earliest dorsoventral asymmetry of *bmp2b* expression in zebrafish. *Development*. 2003; 130:3639–3649. [PubMed: 12835381]
21. Kerscher O, Felberbaum R, Hochstrasser M. Modification of proteins by ubiquitin and ubiquitin-like proteins. *Annu. Rev. Cell Dev. Biol*. 2006; 22:159–180. [PubMed: 16753028]
22. Muratani M, Tansey WP. How the ubiquitin-proteasome system controls transcription. *Nat. Rev. Mol. Cell Biol*. 2003; 4:192–201. [PubMed: 12612638]
23. Pickart CM, Fushman D. Polyubiquitin chains: polymeric protein signals. *Curr. Opin. Chem. Biol*. 2004; 8:610–616.
24. Fekany-Lee K, Gonzalez E, Miller-Bertoglio V, Solnica-Krezel L. The homeobox gene *bozozok* promotes anterior neuroectoderm formation in zebrafish through negative regulation of BMP2/4 and Wnt pathways. *Development*. 2000; 127:2333–2345. [PubMed: 10804176]
25. Melby AE, Beach C, Mullins M, Kimelman D. Patterning the early zebrafish by the opposing actions of *bozozok* and *vox/vent*. *Dev. Biol*. 2000; 224:275–285. [PubMed: 10926766]
26. Kawahara A, Wilm T, Solnica-Krezel L, Dawid IB. Antagonistic role of *vega1* and *bozozok/dharma* homeobox genes in organizer formation. *Proc. Natl. Acad. Sci. USA*. 2000; 97:12121–12126. [PubMed: 11050240]
27. Kawahara A, Wilm T, Solnica-Krezel L, Dawid IB. Functional interaction of *vega2* and *goosecoid* homeobox genes in zebrafish. *Genesis*. 2000; 28:58–67. [PubMed: 11064422]
28. Gonzalez EM, et al. Head and trunk in zebrafish arise via coinhibition of BMP signaling by *bozozok* and *chordino*. *Genes Dev*. 2000; 14:3087–3092. [PubMed: 11124801]
29. Shimizu T, Yamanaka Y, Nojima H, Yabe T, Hibi M, Hirano T. A novel repressor-type homeobox gene, *ved*, is involved in *dharma/bozozok*-mediated dorsal organizer formation in zebrafish. *Mech. Dev*. 2002; 118:125–138. [PubMed: 12351176]
30. Sirotkin HI, Dougan ST, Schier AF, Talbot WS. *bozozok* and *squint* act in parallel to specify dorsal mesoderm and anterior neuroectoderm in zebrafish. *Development*. 2000; 127:2583–2592. [PubMed: 10821757]
31. Ro H, Soun K, Kim EJ, Rhee M. Novel vector systems optimized for injecting in vitro-synthesized mRNA into zebrafish embryos. *Mol. Cells*. 2004; 17:373–376. [PubMed: 15179057]
32. Robu ME, Larson JD, Nasevicius A, Beiraghi S, Brenner C, Farber SA, Ekker SC. p53 activation by knockdown technologies. *PLoS Genet*. 3:e78. [PubMed: 17530925]
33. Onichtchouk D, et al. The *Xvent-2* homeobox gene is part of the BMP-4 signalling pathway controlling dorsoventral patterning of *Xenopus* mesoderm. *Development*. 1996; 122:3045–3053. [PubMed: 8898218]
34. Melby AE, Clements WK, Kimelman D. Regulation of dorsal gene expression in *Xenopus* by the ventralizing homeodomain gene *vox*. *Dev. Biol*. 1999; 221:293–305. [PubMed: 10395789]
35. Trindade M, Tada M, Smith JC. DNA-binding specificity and embryological function of *Xom* (*Xvent-2*). *Dev. Biol*. 1999; 216:442–456. [PubMed: 10642784]
36. Imai Y, et al. The homeobox genes *vox* and *vent* are redundant repressors of dorsal fates in zebrafish. *Development*. 2001; 128:2407–2420. [PubMed: 11493559]
37. Nasevicius A, Ekker SC. Effective targeted gene 'knockdown' in zebrafish. *Nat. Genet*. 2000; 2:216–220. [PubMed: 11017081]

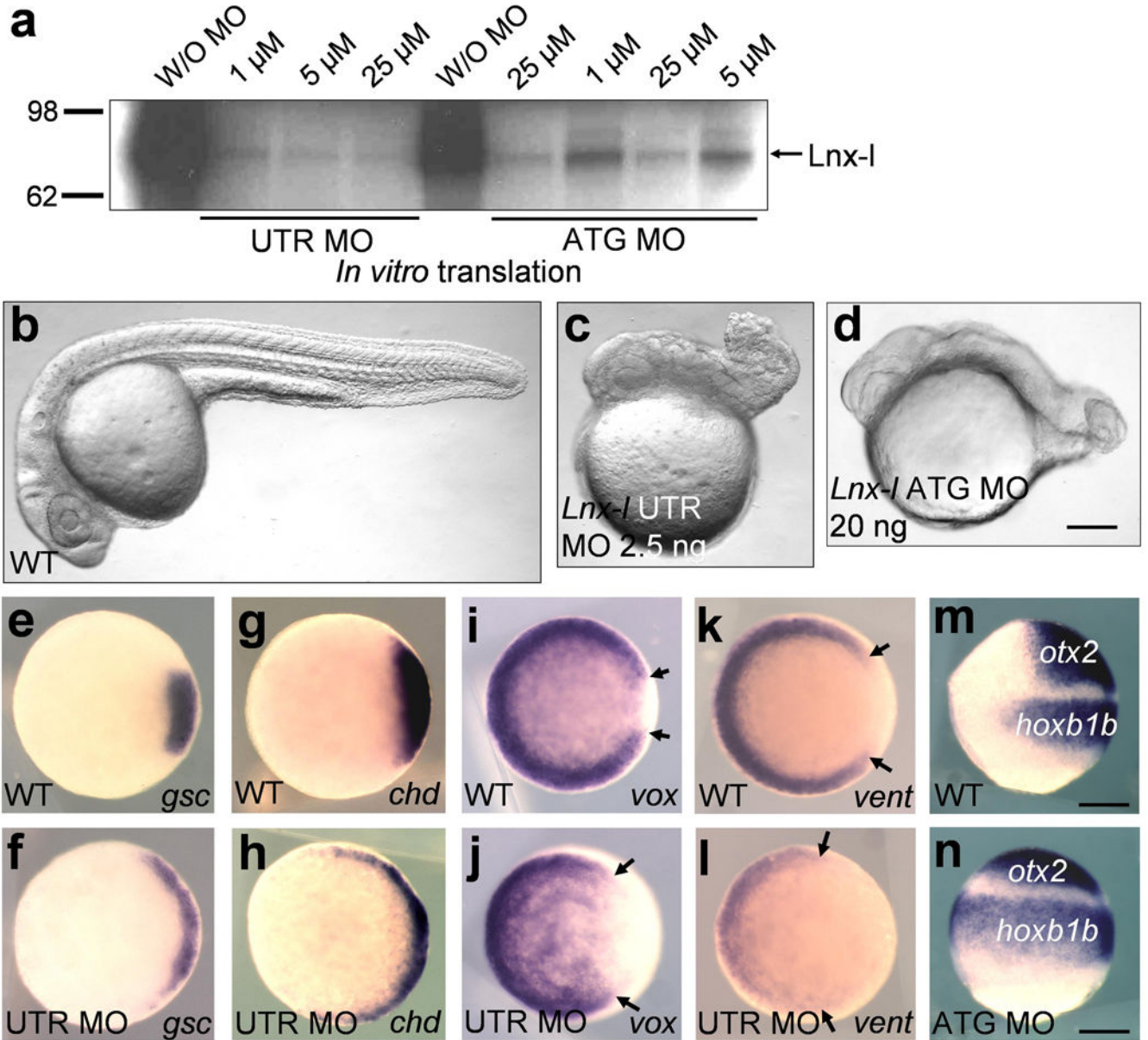


**Figure 1. Depletion of *lnx-1* causes dorsalization**

**a**, Both MOs inhibit *in vitro* translation of *lnx-1* mRNA; *lnx-1* UTR MO is more efficient than ATG MO. **b–d**, *lnx-1* UTR MO (2.5 ng) and ATG MO (20 ng) both caused similar embryonic defects displaying degenerated tail and trunk; 26 hpf embryos, lateral views. **e–l**, *lnx-1* morphants (UTR MO, 2.5 ng) show ventro-laterally expanded expression of *gsc* (**f**) and *chd* (**h**), and reduced expression of *vox* (**j**) and *vent* (**l**), with arrows indicating enlarged dorsal gap in the *vox* and *vent* domains; germ ring stage, animal pole views. **m and n**, *lnx-1* ATG MO (20 ng) injected embryos showed extended expression of *otx2* and *hoXB1b*; 80% epiboly stage, lateral view, dorsal is to the right. Scale bar, 200  $\mu$ m.

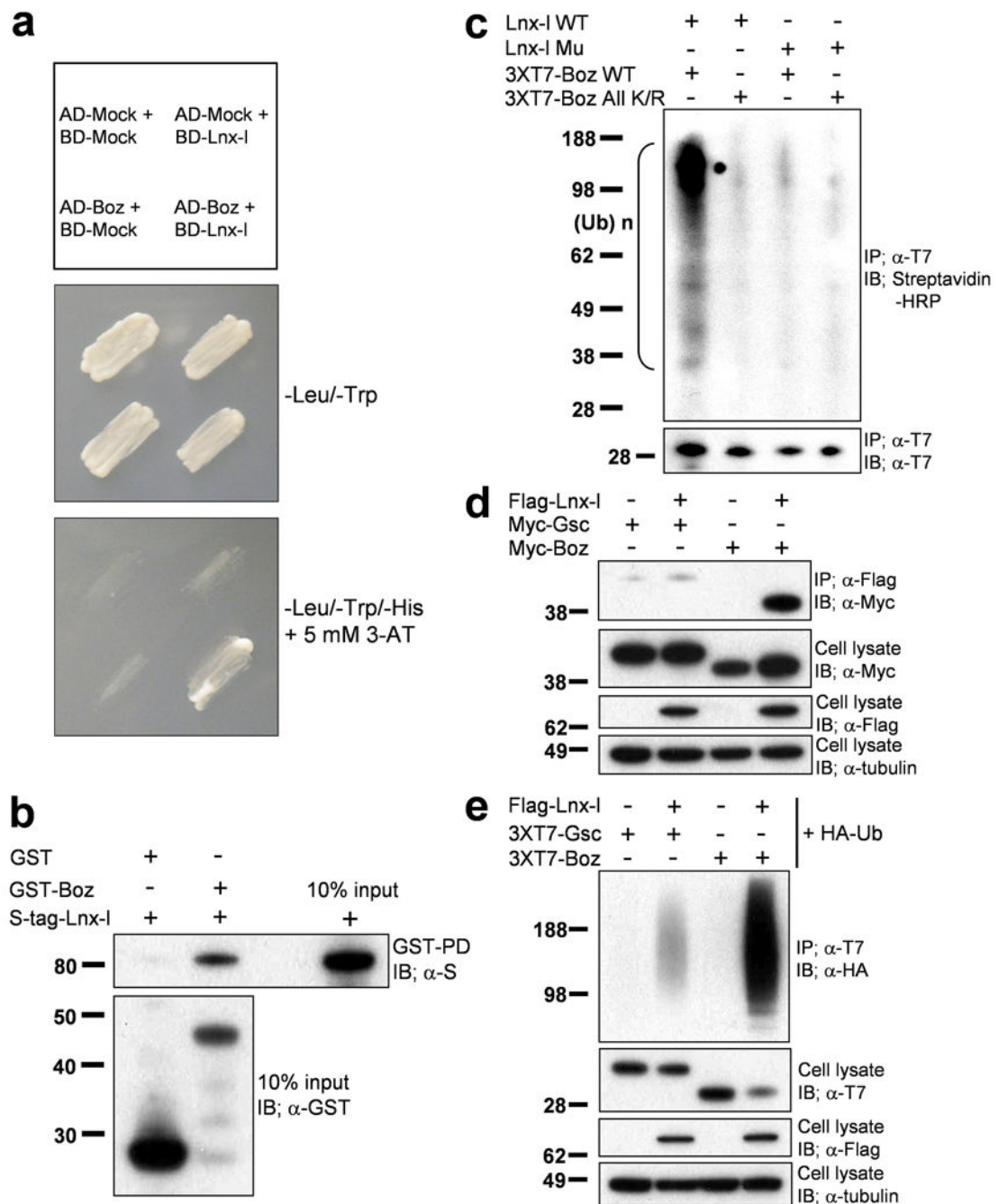


**Figure 2. Lnx-I binds and ubiquitinates Boz but not Gsc**

**a**, Lnx-I-Boz interaction in yeast. Yeast cells were cotransformed with the indicated fusion constructs (upper panel; see Methods). The transformants were plated on  $-Leu/-Trp$  drop-out plates (middle panel) for 3 days. Individual transformants were transferred to  $-Leu/-Trp/-His$  drop-out plates containing 5 mM 3-AT, and incubated for 4 days (bottom panel). Only Boz-Lnx-I co-transformants showed substantial growth, indicating interaction between the two proteins. **b**, Direct interaction between Lnx-I and Boz was confirmed by the GST-pull down assay with proteins purified from bacteria (see Methods); GST alone could not pull-down S-

tagged Lnx-1. **c**, *In vitro* ubiquitination assay was performed as described in Methods. Wt Boz mixed with extracts containing Wt Lnx-1 yielded abundant ubiquitinated products, while RING mutant Lnx-1 did not ubiquitinate Wt Boz, and Wt Lnx-1 did not ubiquitinate Boz All K/R. **d**, Lnx-1 interacts with Boz but not with Gsc. Flag-tagged Lnx-1 was cotransfected into 293T cells with 6xMyc-tagged Gsc or Boz. After 48 h, IP and IB were performed with the indicated antibodies. **e**, Lnx-1 ubiquitinates Boz but not Gsc. Flag-tagged Lnx-1 was cotransfected with 3xT7 tagged Gsc or Boz. The yield of polyubiquitinated Gsc is very low compared to that of Boz (see also Fig. 3, below)..  $\alpha$ -tubulin was used as loading control.

Author Manuscript

Author Manuscript

Author Manuscript

Author Manuscript

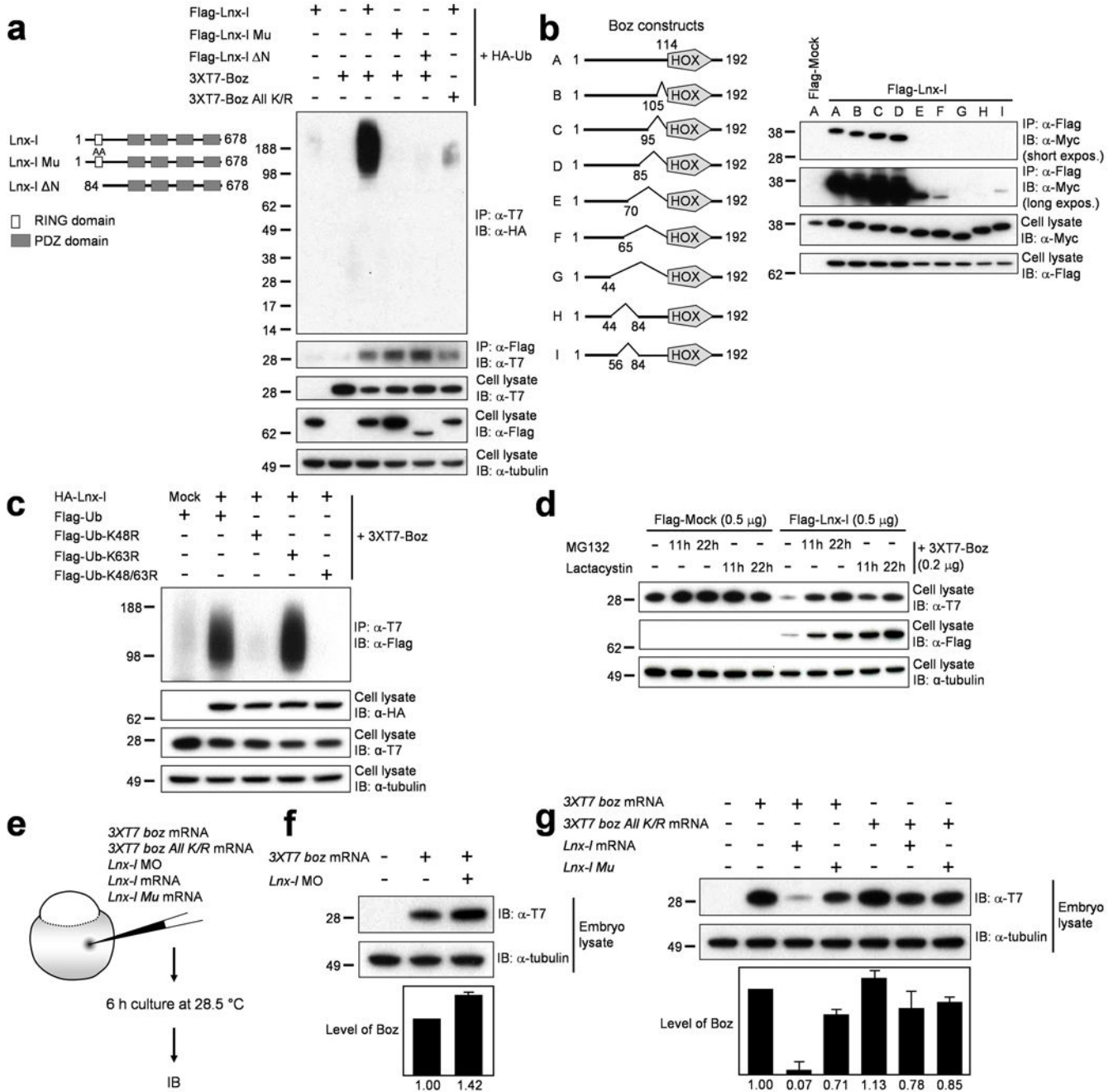


**Figure 3. Lnx-1-mediated polyubiquitination destabilizes Boz**

**a**, Flag-tagged Lnx-1, 3xT7-Boz, and HA-ubiquitin were cotransfected into 293T cells as indicated. Lnx-1 constructs are shown on the left. Only Wt Boz is significantly polyubiquitinated by Wt Lnx-1. Molecular size markers are indicated at the left. **b**, Schematic diagrams of Boz deletion constructs are shown at the left. 6xMyc epitope-tagged Boz constructs were cotransfected with Flag-Lnx-1. Upon IP with anti-Flag antibody, the coprecipitates were subjected to IB with anti-Myc antibody. Short and long exposures are shown to illustrate the range of interaction strength between Lnx-1 and Boz. **c**, HA-tagged

Lnx-1 and 3xT7-tagged Boz were cotransfected with Flag-tagged Wt or mutant ubiquitin. The K48R ubiquitin mutant could not support Boz polyubiquitination. **d**, Transfected cells were incubated with MG132 or lactacystin, each at 10  $\mu$ molar, for the indicated times. Destabilization of Boz by Lnx-1 cotransfection was inhibited by MG132 or lactacystin. Lnx-1 itself was stabilized in a time-dependent manner by the proteasome inhibitors. **e**, Schematic diagram of experimental design in **(f)** and **(g)**. **f**, 20 pg of 3xT7 *boz* mRNA was injected with or without 2.5 ng of *lnx-1* UTR MO. Depletion of endogenous Lnx-1 increased Boz levels. **g**, 20 pg 3xT7 *boz* or 3xT7 *boz All K/R* mRNA was injected with 50 pg *lnx-1* or 50 pg *lnx-1 Mu* mRNA. Wt Lnx-1 strongly destabilizes Wt Boz. Error bars in **f** and **g** were obtained from two repeats each of two independent experiments.  $\alpha$ -tubulin was used as loading control.

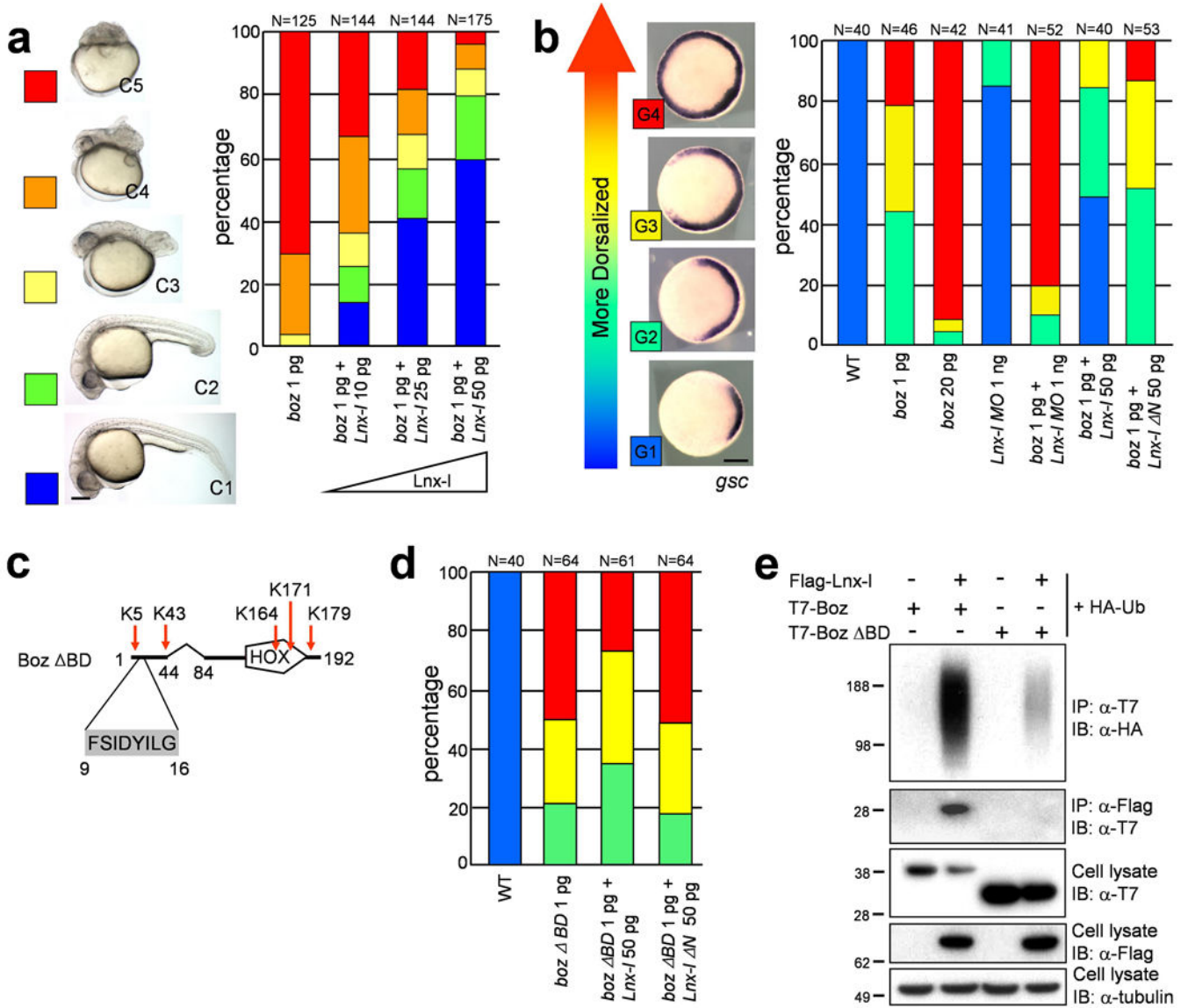


**Figure 4. *Lnx-I* counteracts *Boz*-mediated dorsalization**

**a, b, d**, The amounts of injected RNA or MO are shown beneath each bar, and number of embryos above each bar. **a**, Coinjection of *lnx-I* mRNA rescues *boz*-induced dorsalization. The embryonic morphology was classified as C1-C5 at 26 hpf, as illustrated at the left. **b**, Dorsalization was analyzed by observing the domain of *gsc* expression at the germ ring stage. *Boz* and *lnx-I* MO show synergism, while *lnx-I* mRNA counteracts dorsalization. **c**, Schematic drawing of *Boz* lacking the *Lnx-I* binding domain (*Boz* ΔBD), but retaining the Goosecoid-Engrailed homology domain (amino acid 9–16) and all lysine residues. **d** The *gsc* expression level, analyzed as in **b**, shows that *Boz* ΔBD is resistant to *Lnx-I* (compare to **b**). **e**, T7 epitope-tagged Wt *Boz* or *Boz* ΔBD was cotransfected into 293T cells with Flag-*Lnx-I* and HA-Ub. *Boz* ΔBD ubiquitination is almost absent. Scale bar, 200 μm.

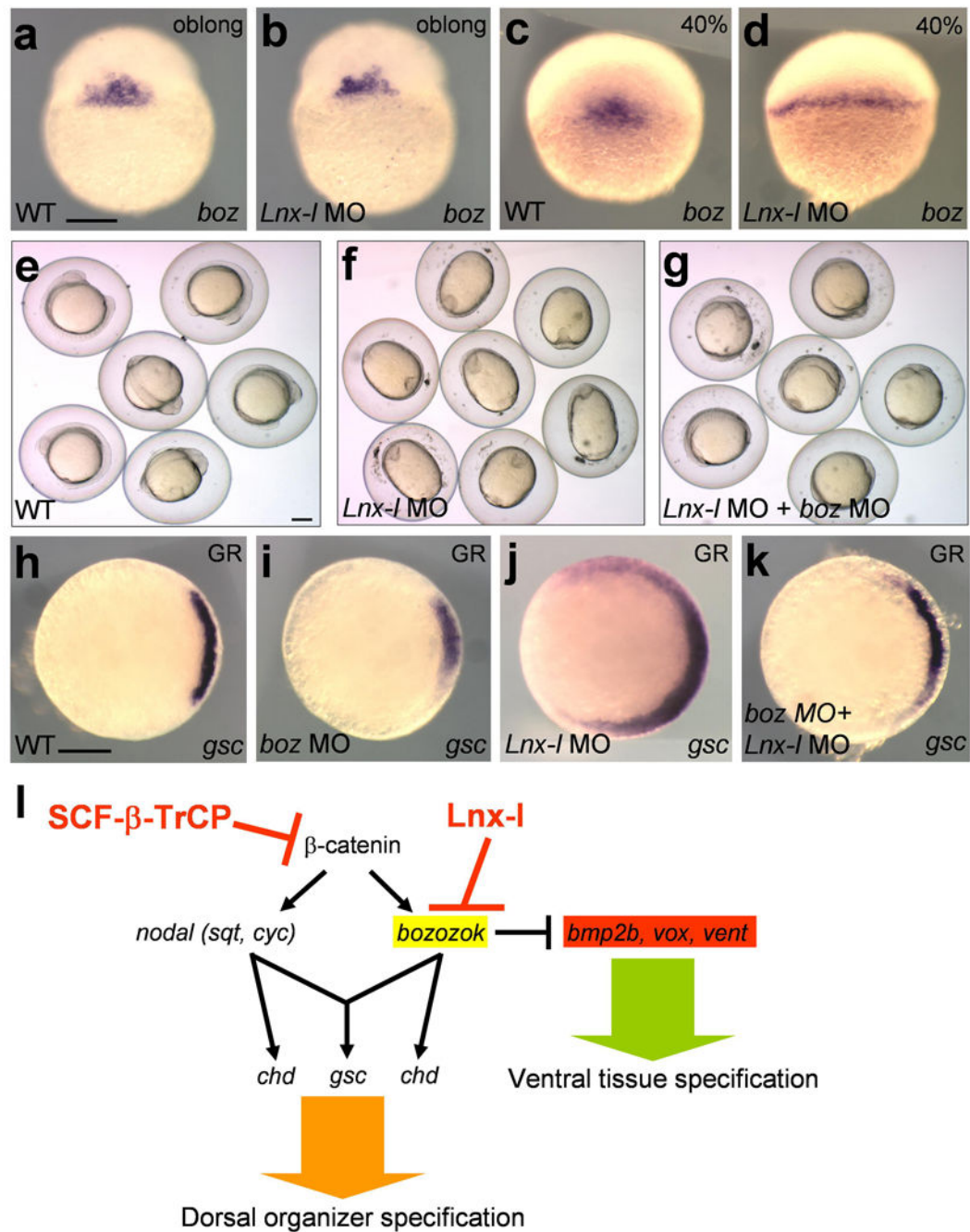


**Figure 5. Boz depletion mitigates dorsalization in *lnx-1* morphants**

**a–d**, *lnx-1* morphants showed normal expression of *boz* at the oblong stage (30/30), but in some morphants, *boz* expression was expanded laterally at 40% epiboly (12/31); 2.5 ng *lnx-1* UTR MO was injected into each embryo in **b** and **d**. **e–g**, 5-somite stage. **e**, Uninjected control. **f**, Embryos injected with 20 ng *lnx-1* ATG MO; the oval shape indicates dorsalization (92%, N=100). **g**, *boz* MO (5 ng), injected together with 20 ng *lnx-1* ATG MO, alleviated the morphological defects of *lnx-1* depletion (37% dorsalized, N=116). **h–k**, *gsc* expression in embryos injected with indicated MOs. **h**, uninjected. **i**, 5 ng of *boz* MO. **j**, 2.5

ng *lnx-1* UTR MO (89% expanded *gsc* expression, N=28). **k**, 2.5 ng *lnx-1* UTR MO plus 5 ng *boz* MO (32% expanded *gsc* expression, N=28). **l**, A schematic model of the role of Lnx-1 during establishment of the D–V body axis. Scale bar, 200  $\mu$ m.

Author Manuscript

Author Manuscript

Author Manuscript

Author Manuscript